

This is the accepted manuscript made available via CHORUS. The article has been published as:

5f delocalization-induced suppression of quadrupolar order in $\text{U}(\text{Pd}_{1-x}\text{Pt}_x)_3$

H. C. Walker, M. D. Le, K. A. McEwen, M. Bleckmann, S. Süllow, C. Mazzoli, S. B. Wilkins,
and D. Fort

Phys. Rev. B **84**, 235142 — Published 27 December 2011

DOI: [10.1103/PhysRevB.84.235142](https://doi.org/10.1103/PhysRevB.84.235142)

5f delocalisation induced suppression of quadrupolar order in $\text{U}(\text{Pd}_{1-x}\text{Pt}_x)_3$

H. C. Walker,^{1,2} M. D. Le,^{3,2} K. A. McEwen,² M. Bleckmann,⁴ S. Süllow,⁴ C. Mazzoli,¹ S. B. Wilkins,^{5,1} and D. Fort⁶

¹*European Synchrotron Radiation Facility, Boîte Postale 220, 38043 Grenoble, France*

²*London Centre for Nanotechnology, and Department of Physics and Astronomy,
University College London, 17-19 Gordon Street, London WC1H 0AH, UK*

³*Helmholtz-Zentrum-Berlin für Materialien und Energie,
Hahn-Meitner Platz 1, D-14109 Berlin, Germany*

⁴*Institute for Physics of Condensed Matter, TU Braunschweig, 38106 Braunschweig, Germany*

⁵*Brookhaven National Laboratory, Condensed Matter Physics and
Material Science Department, Bldg #501B, Upton, NY 11973-5000, USA*

⁶*Department of Metallurgy and Materials Science,
University of Birmingham, Birmingham B15 2TT, UK*

(Dated: November 10, 2011)

We present bulk magnetic and transport measurements and X-ray resonant scattering measurements on $\text{U}(\text{Pd}_{1-x}\text{Pt}_x)_3$ for $x = 0.005$ and 0.01 , which demonstrate the high sensitivity of the quadrupolar order in the canonical antiferroquadrupolar ordered system UPd_3 to doping with platinum. Bulk measurements for $x = 0.005$ reveal behaviour similar to that seen in UPd_3 , albeit at a lower temperature, and X-ray resonant scattering provides evidence of quadrupolar order described by the Q_{xy} order parameter. In contrast, bulk measurements reveal only an indistinct transition in $x = 0.01$, consistent with the observation of short range quadrupolar order in our X-ray resonant scattering results.

PACS numbers: 75.25.Dk, 75.40.Cx, 78.70.Ck

I. INTRODUCTION

The extended nature of the 5f radial wavefunction, relative to that of the 4f, leads to the possibility of greater hybridisation with valence and conduction electrons. Depending on the actinide element, the interactinide spacing and the actinide environment, actinide compounds can possess properties ranging from those of itinerant transition metal-like systems to those of localised rare-earth-like systems, such that they present a forum for investigating physics at the cross-over from itinerant to localised electrons. The 5f electrons in the vast majority of uranium intermetallic compounds are considered to be itinerant, or partially itinerant¹, but UPd_3 presents a rare exception to this rule. The double-hexagonal close-packed crystal structure (TiNi_3 -type, space group $\#194 P6_3/mmc$) results in an inter-uranium spacing of 4.106 \AA , i.e. greater than the Hill limit² of 3.5 \AA , and consistent with the 5f electrons being fully localised, as evident from the observation of well defined crystal field excitations^{3,4}. However, the Hill criterion can only be used as an indication that the 5f electrons may be localised, and is not always valid. If we change the ligand by moving down the same group of the periodic table, replacing platinum for palladium, we find that despite the inter-uranium distance being little changed at 4.132 \AA , and the crystal structure only slightly modified to hexagonal close-packed, the electronic properties are very different: UPt_3 is a heavy fermion superconductor⁵, in which at least one f -electron is itinerant¹. This difference arises from the 5d valence electrons in UPt_3 being less tightly bound than those of the Pd 4d electrons, resulting in a greater degree of fd hybridisation and hence

delocalisation of the f electrons⁶.

Bulk measurements (ultrasound⁷, heat capacity⁸⁻¹⁰, magnetic susceptibility^{9,11}, thermal expansion and magnetostriction¹²) reveal that UPd_3 undergoes four successive phase transitions below 8 K , which have been identified through X-ray resonant scattering studies as relating to the antiferroquadrupolar order of the $5f^2$ electrons on the quasi-cubic uranium sites^{4,10,13,14}. The four transitions: $T_0 = 7.8 \text{ K}$, $T_{+1} = 6.9 \text{ K}$, $T_{-1} = 6.7 \text{ K}$ and $T_2 = 4.4 \text{ K}$ can be explained by a crystal field model requiring a doublet ground state on the quasi-cubic sites¹⁵. The primary order parameter of the phase below T_0 is Q_{zx} , with an anti-phase stacking of the quadrupoles along the c -axis, indicated by a (103) superlattice reflection indexed in the low temperature orthorhombic unit cell¹⁶. The primary Q_{zx} order parameter is accompanied by a secondary $Q_{x^2-y^2}$ order parameter as the matrix elements of both share the same symmetry^{4,10}. The narrow temperature range between T_{+1} and T_{-1} and difficulty in stabilizing a displex cryostat within this interval means that it has not been possible to perform azimuthal measurements in this phase. However, in temperature dependent measurements, we observed the emergence of a (104) superlattice reflection only below the T_{-1} transition¹³. In combination with the small change in the magnetic entropy, as obtained from heat capacity measurements, this is consistent with the onset at T_{+1} of a Q_{yz} component to the quadrupolar order, with an anti-phase stacking along the c -axis. A recent analysis¹⁴ of the two phases below T_{-1} revealed that these phase transitions are associated with the onset of an in-phase stacking Q_{xy} component together with an induced secondary Q_{yz} component, the ratio of which changes at the T_2 transition. This be-

haviour is consistent with the large entropy change at T_{-1} .

In an attempt to understand the origins of the quadrupolar order in UPd_3 there have been several experiments investigating its fragility to chemical pressure. Recently we have substituted neptunium for uranium and found that bulk measurements imply that quadrupolar order is still present in solid solutions containing up to 5% neptunium¹⁷. Meanwhile, the majority of experiments investigating the alloying of platinum for palladium have concentrated on the opposite end of the phase diagram, to determine the sensitivity of the superconductivity and magnetism of UPt_3 to Pd doping^{18–22}. The superconductivity is found to be highly sensitive, being suppressed by only 0.5% Pd²², whilst the small moment magnetic order is suppressed with 1% Pd²¹. In contrast, little work has been done at the Pd rich end of the phase diagram. Zochowski et al.¹² have shown that in thermal expansion experiments 5% Pt is sufficient to suppress the antiferroquadrupolar order, but no measurements with more dilute Pt dopings have been published.

In this paper on $\text{U}(\text{Pd}_{1-x}\text{Pt}_x)_3$ we present a comprehensive set of bulk property and X-ray resonant scattering experimental results for $x = 0.005$ and 0.01 revealing the sensitivity of the quadrupolar order to increasing fd hybridisation.

II. BULK MEASUREMENTS

The single crystal samples of $\text{U}(\text{Pd,Pt})_3$ with 0.5% and 1% Pt, used in all measurements, were grown at the University of Birmingham using the tri-arc Czochralski pulling method²³ starting with stoichiometric amounts of 3N uranium and 4N palladium and platinum metals.

A. Heat capacity

Heat capacity measurements were performed using the standard heat pulse technique in a Quantum Design Physical Properties Measurement System with an optional ^3He insert. The sample masses were 46.88 mg ($x = 0.01$) and 54.61 mg ($x = 0.005$). The magnetic heat capacity was obtained by subtracting the heat capacity of ThPd_3 , an isostructural phonon blank¹⁰. Figure 1(a) compares C/T for the two doped compounds with that of pure UPd_3 . The data for $x = 0.005$ bear a resemblance to the results for UPd_3 , in that there is a lambda-type anomaly, although at a reduced temperature of $T = 4.5$ K, which we may associate with the T_{-1} transition in pure UPd_3 . In addition there is a weak shoulder at $T = 2.5$ K, which we might ascribe to T_2 , but there is no evidence of a T_0 shoulder above the lambda anomaly. Furthermore, we observed that the lambda anomaly clearly moves to higher temperatures in increasing magnetic fields, see Fig. 1(b), which is similar to the behaviour of UPd_3 for applied fields in the basal

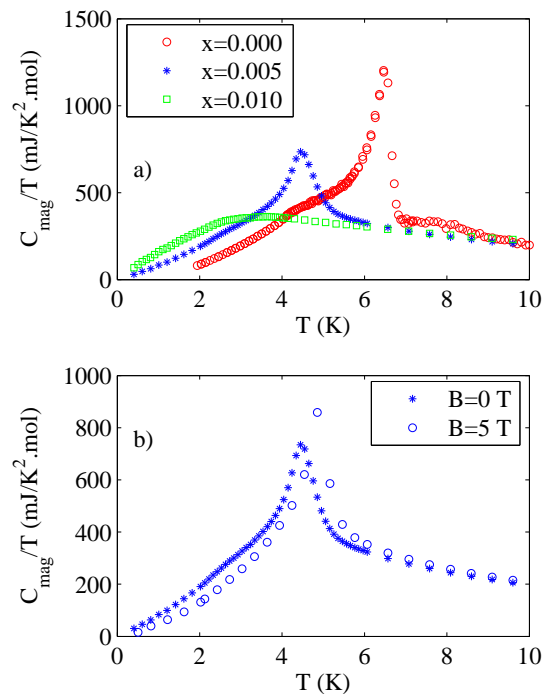


FIG. 1: (a) Temperature dependence of the magnetic C/T for $\text{U}(\text{Pd}_{1-x}\text{Pt}_x)_3$ with $x = 0, 0.005, 0.01$ and (b) for $x = 0.005$ in zero magnetic field and $B = 5$ T, where the magnetic field is applied along the a -axis. The UPd_3 data is taken from Walker *et al.*¹⁰.

plane. The data for $x = 0.01$ are more strongly contrasting, with only a broad hump at $T = 2.7$ K, more similar to that seen in $(\text{U}_{0.95}\text{Np}_{0.05})\text{Pd}_3$ ¹⁷, and which may be indicative of only a short range order.

Based on the similarities in the form of the heat capacity for $x = 0$ and $x = 0.005$, we have attributed the two anomalies in the $x = 0.005$ data as arising from quadrupolar transitions, where the unusual magnetic field behaviour for an antiferroquadrupolar ordered state is due to the strong anisotropies present in the system, which allows a magnetic field in some directions both to reinforce the antiferroquadrupolar ordered structure and lower the anisotropy energy for certain quadrupolar order parameters. Moreover, the similarities of the magnetic field dependence observed for $x = 0.005$ and for $x = 0$ suggest that both the crystal field and the exchange interactions causing the anisotropies in UPd_3 are relatively unchanged with small Pt doping.

The magnetic entropy calculated from this data indicates that S_{mag} is reduced with increasing Pt doping. Quantitatively, at T_{-1} for $x = 0.005$ only 70% and for $x = 0.01$ only 30% of the entropy is reached compared to UPd_3 .

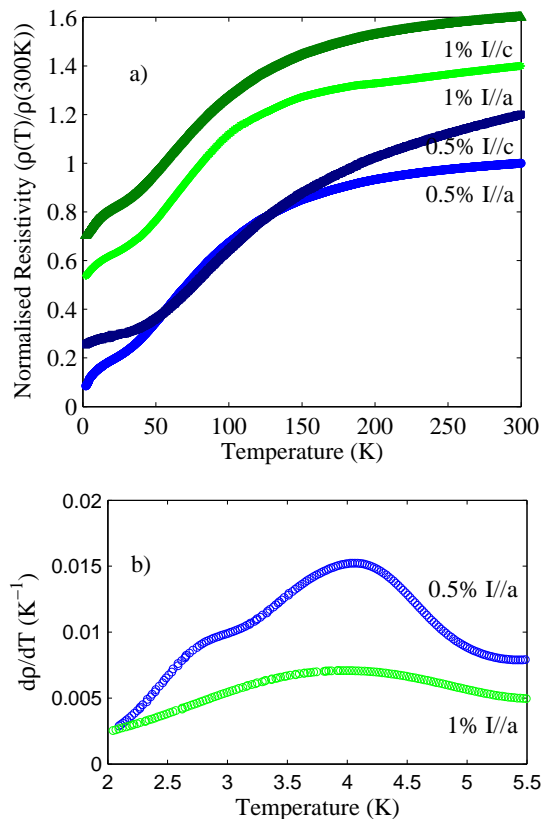


FIG. 2: (a) Normalised resistivity $\rho(T)/\rho(300K)$ (with an offset of 0.2 units between successive curves) and (b) temperature derivative of the normalised resistivity of $U(Pd_{1-x}Pt_x)_3$ for $x = 0.005, 0.01$.

B. Electrical Resistivity

Resistivity measurements were performed using a standard four point contact technique in a ⁴He cryostat in zero magnetic field, with two different orientations $I//a$ and $I//c$. The data shown in Fig. 2(a) has been normalised to the room temperature resistivity, which for each set of measurements was of the order of $\sim 130\mu\Omega$ cm. On taking the temperature derivative of the resistivity, fig. 2(b), for $x = 0.005$ two clear features are seen: a shoulder and a peak. These are reminiscent of the features corresponding to phase transitions observed in the heat capacity data. The derivative with respect to temperature for $x = 0.01$ shows no clear anomaly that could be associated with a transition, and is again similar to the form of the heat capacity.

C. Magnetic Susceptibility

The temperature dependence of the magnetic susceptibility was measured using single crystal samples of $U(Pd_{1-x}Pt_x)_3$ with $x = 0.005, 0.01$ for a magnetic field of 0.01 T applied along both the a and c -axes using a

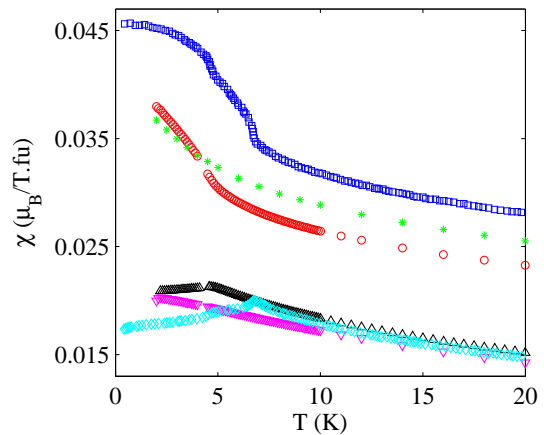


FIG. 3: Magnetic susceptibility of $U(Pd_{1-x}Pt_x)_3$ with $x = 0.005$ (\circ \triangle), 0.01 (\ast ∇) measured as a function of temperature with a field of 0.01 T applied along the a and c -axes respectively. Also shown for comparison is the magnetic susceptibility of UPd_3 for $H//a$ (\square) and $//c$ (\diamond) taken from McEwen et al.¹¹.

commercial SQUID magnetometer. In the paramagnetic phase the data are very similar for the two different compositions, showing a comparable anisotropy. On inspection of the low temperature data shown in Figure 3(a), one can identify one transition for each sample doping. For $x = 0.005$ there is a maximum in the data for $B//c$ and an inflexion point in that for $B//a$ at $T = 4.6$ K, consistent with the higher temperature quadrupolar transition, T_{-1} , obtained from the heat capacity data. However, no additional features are observed in the susceptibility which might be associated with the lower temperature T_2 transition seen in the heat capacity. Further evidence for associating the anomalies with the T_{-1} transition comes from their form, i.e. the rapid increase in the susceptibility of the 0.5% Pt sample for $B//a$, due to a mixing of the ground and first excited crystal field levels²⁴, accompanied by a sharp peak for $B//c$, is strongly reminiscent of the features seen in pure UPd_3 ¹¹. Meanwhile, for $x = 0.01$ there is a very small maximum for $B//c$ at $T = 2.1$ K.

III. X-RAY RESONANT SCATTERING MEASUREMENTS

X-ray resonant scattering (XRS) occurs when the incident photon energy is equal to the energy difference between the ground state and some intermediate state, making it an experimental probe of the sensitivity of these states to magnetic or higher order multipolar interactions. Thus, unlike neutrons which can only couple to the induced lattice distortions, XRS allows us to probe quadrupolar order directly, through a study of the energy, polarisation and azimuthal dependence of the intensities of the superlattice reflections. The power of

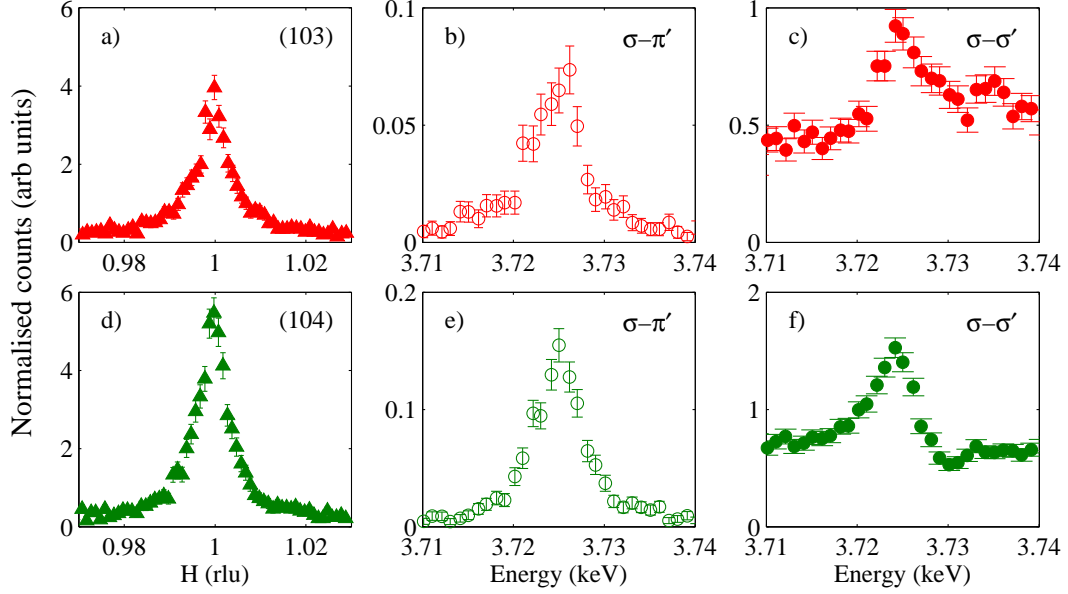


FIG. 4: Reciprocal space h-scans through the reflections (a) (103) and (d) (104) with no polarisation analysis; and the energy dependence of the same reflections (b,c) and (e,f) in $\sigma - \pi'$ and $\sigma - \sigma'$ respectively, at $T = 2$ K in $\text{U}(\text{Pd}_{0.995}\text{Pt}_{0.005})_3$.

this technique to differentiate between different types of quadrupolar order has been successfully demonstrated for UPd_3 ^{10,14}.

Experiments were performed on the ID20 magnetic scattering beamline²⁵ at the European Synchrotron Radiation Facility, using a monochromatised X-ray beam with an energy of 3.726 keV, the uranium M_{IV} absorption edge, where electric dipole transitions connect the core $3d_{3/2}$ states to $5f$ states. The samples were oriented with a Laue camera, cut and then polished using $0.25\mu\text{m}$ diamond paste. They were mounted in a displax cryostat (base temperature ≈ 2 K), to give a vertical scattering plane defined by the $[001]$ and $[100]$ directions. Polarisation analysis was undertaken using a high quality Au (111) single crystal.

A. $x=0.005$

At $T = 2$ K the UB matrix was refined, returning the orthorhombic cell lattice parameters of the 0.5%Pt sample: $a = 9.950$ Å, $b = 5.730$ Å and $c = 9.648$ Å. Using $E_i = 3.726$ keV and no polarisation analysis, well-defined peaks were observed at both the (103) and (104) superlattice reflections, see Fig. 4. The energy resonances in $\sigma - \pi'$ and $\sigma - \sigma'$ also shown in Fig. 4 clearly demonstrate that the two reflections are related to the ordering of the uranium $5f$ electrons, and the presence of a resonance in $\sigma - \sigma'$ excludes the possibility of the scattering arising from dipolar (magnetic) long range order. The $\sigma - \sigma'$ resonances sit on a sizeable background, which is absent in $\sigma - \pi'$. We conclude that the background arises from the modulated lattice distortion induced by the quadrupolar

order. A similar background in the $\sigma - \sigma'$ channel has been seen for pure UPd_3 ²⁶.

The temperature dependence of the unpolarised scattering from the two different reflections was obtained by fitting a lorentzian peak shape to individual theta rocking scans, (where θ is the angle between the incident beam and the planes normal to the scattering vector). The results shown in Fig. 5(a) indicate that the behaviour is very similar for the two reflections with a transition temperature of ~ 4 K. The transition appears to be sharper for (104), whilst there might be some critical scattering for (103). The temperature dependence of the (103) superlattice reflection was further investigated by using the polarisation analyser to separate the $\sigma - \sigma'$ and $\sigma - \pi'$ scattering. Intriguingly figure 5(b) suggests that there are two different transition temperatures for $\sigma - \sigma'$ and $\sigma - \pi'$. This might indicate a further transition, where the relative magnitudes of the different quadrupolar order parameters have changed subtly.

Careful examination of the (103) peak data near the 4K transition reveals that long range ordering develops at 4.2 K, whilst the (104) peak only appears at 4.1 K. This is analogous to the T_0 and T_{-1} transitions in UPd_3 , save that in UPd_3 , the two transitions are separated by 1.1 K¹⁰, rather than 0.1 K as in this case. We interpret the 4.2 K transition as being to an anti-phase stacking of the $5f$ quadrupoles along the c -axis, and the 4.1 K transition to a combination of this and an inphase stacking.

Heat capacity measurements in section IIA suggest that there is another transition at ~ 2.7 K, similar to the T_2 transition in UPd_3 . However, no clear anomaly is seen in the XRS data (Fig. 5) at this temperature, although this is close to the base temperature limit attainable for

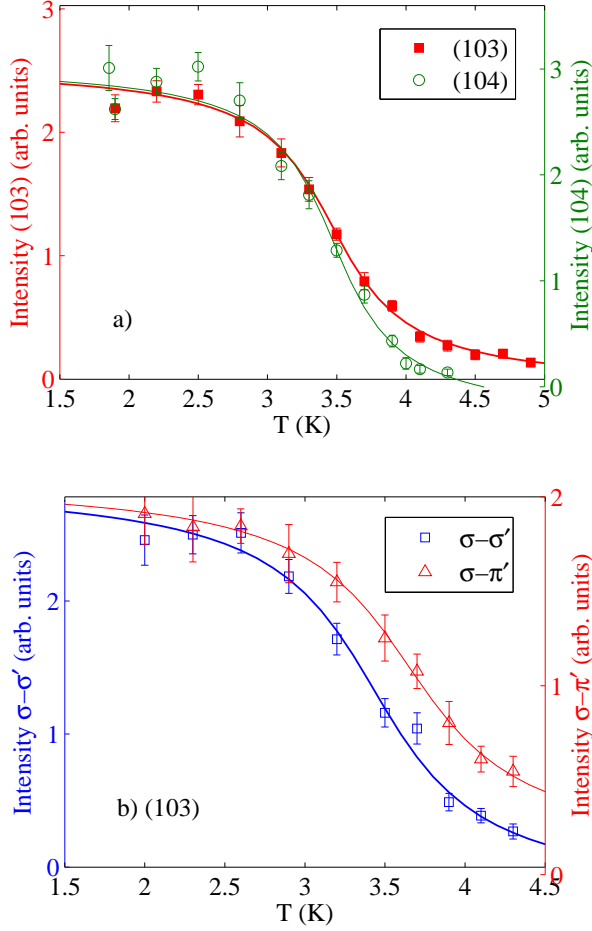


FIG. 5: (a) Temperature dependence of the integrated intensity of the total scattering from the (103) and (104) reflections in $\text{U}(\text{Pd}_{0.995}\text{Pt}_{0.005})_3$ at $\Psi \approx -124^\circ$, and (b) the temperature dependence of the (103) scattering in the $\sigma-\sigma'$ and $\sigma-\pi'$ channels at $\Psi = 54^\circ$. The lines are a guide to the eye.

the cryostat, and it is possible that due to heating by the beam we might not have reached sufficiently low temperatures to enter this phase. Alternatively, it may be that due to insufficient data density we are unable to identify any anomaly, which has previously been found to be very weak at the T_2 transition in the temperature dependence of UPd_3 as measured by X-ray resonant scattering¹³.

In UPd_3 the sharp change in entropy at the T_{-1} transition is associated with the onset of an in-phase component of the quadrupole stacking along the c -axis described by the Q_{xy} order parameter in addition to a Q_{zx} anti-phase ordering. Since the temperature dependence (see Fig. 5(a)) shows the onset of scattering at both reflections at a temperature consistent with the lambda anomaly seen in the heat capacity, to investigate whether the quadrupolar order in $x = 0.005$ can be described similarly, the azimuthal dependence of the scattering from the (104) reflection was measured. This was done by measuring theta rocking curves over the (104) reflection for each

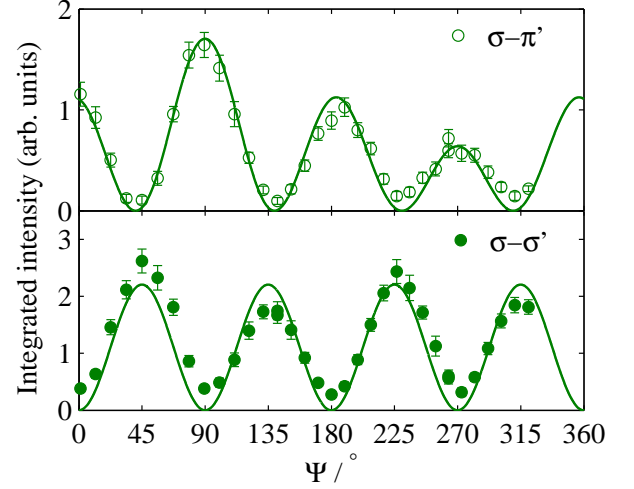


FIG. 6: Azimuthal dependence of the scattering from (104) in the $\sigma-\pi'$ and $\sigma-\sigma'$ channels measured at $T = 2$ K in $\text{U}(\text{Pd}_{0.995}\text{Pt}_{0.005})_3$ with a calculation for Q_{xy} order shown as a solid line.

value of the azimuthal angle Ψ in the rotated ($\sigma-\pi'$) and unrotated ($\sigma-\sigma'$) channels, and then fitting a lorentzian peak profile to obtain the integrated intensity, which was corrected for the variation in the absorption²⁷. The azimuthal angle Ψ is defined relative to the reference vector [010]. The azimuthal dependence of the scattering from the (103) reflection showed a very complex form which may imply an additional ordering of the quadrupoles on the hexagonal sites together with anti-phase stacking of the Q_{zx} and Q_{xy} quadrupoles along the c -direction. The data are similar to the recently measured azimuthal dependence of UPd_3 and will be discussed further in a separate publication.

Figure 6 shows the azimuthal dependence of the (104) intensity in both scattering channels, measured at $T = 2$ K so as to maximise the count rate. There is excellent agreement between the experimental data and the calculation for the Q_{xy} ordering parameter (solid line):

$$I \propto \left| \epsilon' \cdot \begin{pmatrix} 0 & 1 & 0 \\ 1 & 0 & 0 \\ 0 & 0 & 0 \end{pmatrix} \cdot \epsilon \right|^2, \quad (1)$$

where $\epsilon^{(\prime)}$ is the incident (scattered) polarisation state²⁸. For both scattering channels the calculation accurately reproduces the positions of the maxima and minima, which are in antiphase between the channels. In addition the Q_{xy} calculation reproduces the modulation of the maxima for $\sigma-\pi'$. This demonstrates that 0.5% Pt doping, whilst apparently compressing the $T_{+1} < T < T_0$ phase and lowering the temperature range for the $T_2 < T < T_{-1}$ phase, preserves the type of quadrupolar order found in UPd_3 .

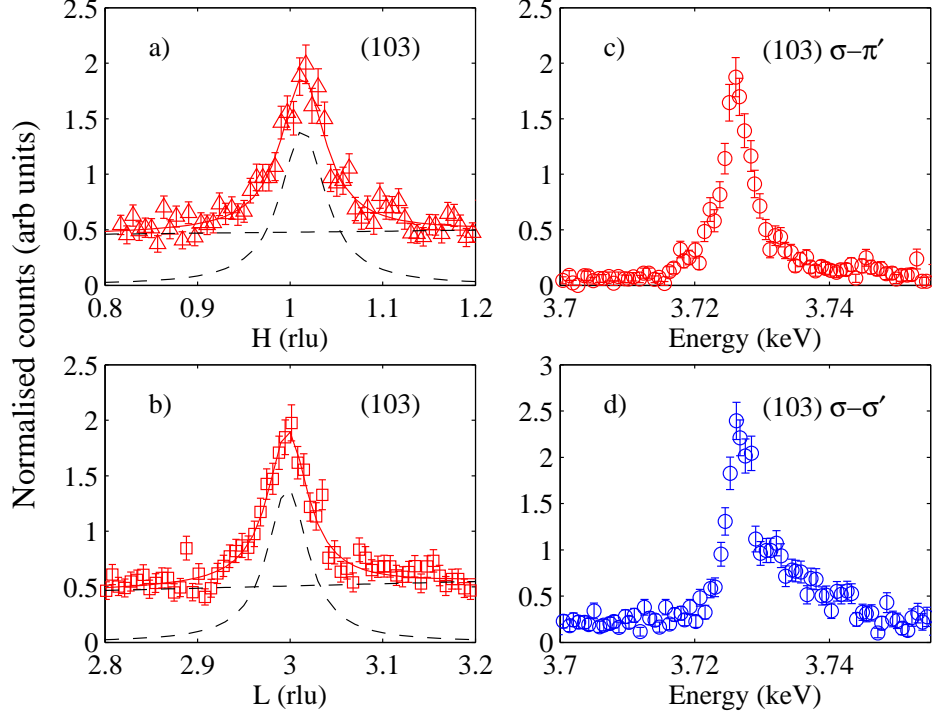


FIG. 7: (a) H and (b) L-scans through the superlattice reflection (103) in the $\sigma - \pi'$ channel and Energy scans in (c) $\sigma - \pi'$ and (d) $\sigma - \sigma'$ in $\text{U}(\text{Pd}_{0.99}\text{Pt}_{0.01})_3$ at $T = 2$ K. The solid lines in panels (a) and (b) correspond to fits to a lorentzian peak shape. A comparison with the H-scans shown in Fig. 4 shows the striking difference between the peak widths for the two dopings.

B. $x=0.01$

On cooling to 2 K, the quality of the $\text{U}(\text{Pd}_{0.99}\text{Pt}_{0.01})_3$ sample was verified by the observation of a well defined sharp peak in the theta rocking curve of the (004) Bragg peak. On refining the UB matrix, the lattice parameters were determined to be $a = 9.935$ Å, $b = 5.732$ Å and $c = 9.651$ Å. We then searched for the (103) and (104) superlattice reflections. No evidence of the (104) reflection was found, but at (103) a weak broad peak was observed in both the $\sigma - \sigma'$ and $\sigma - \pi'$ scattering channels. The energy resonances shown in Figure 7 for this reflection indicate that this superlattice reflection is associated with the ordering of the uranium $5f$ electrons, and hence confirms that the quadrupolar order has not been fully suppressed for 1% Pt doping. The resonances are much cleaner relative to those in Fig. 4, suggesting less interference with any induced lattice distortion. Making a fit using a lorentzian peak profile to the peaks measured in reciprocal space scans along the h and l directions allows the full width half maximum to be determined, and hence the real space correlation length. The fits shown in Figure 7 correspond to a correlation length of 28 ± 3 Å, i.e. the quadrupolar order is only short-range, extending over approximately three unit cells.

We next investigated the temperature dependence of the scattering from the (103) reflection in the $\sigma - \pi'$

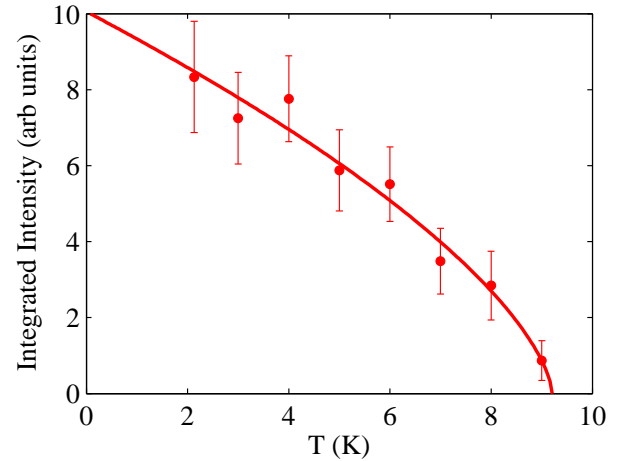


FIG. 8: Temperature dependence of the integrated intensity of the $\sigma - \pi'$ scattering from the reflection (103) in $\text{U}(\text{Pd}_{0.99}\text{Pt}_{0.01})_3$. The solid line corresponds to $I \propto (T - T^*)^\beta$, where $T^* = 9.2 \pm 0.2$ K and $\beta = 0.65 \pm 0.13$.

channel. For each temperature a theta rocking scan was performed, and then by fitting a lorentzian peak profile to each scan, the integrated intensity was obtained as a function of temperature. As can be seen in Fig. 8 there is scattering intensity up to $T^* = 9.2$ K. This is a

very much higher transition temperature than that seen in bulk measurements. However, bulk measurements are likely to be insensitive to such a short range order. It is notable that there is no clear anomaly in this data corresponding to the broad transition seen in bulk measurements at $T \approx 2.7$ K. Unfortunately, the width of the peaks, combined with their low intensity, made it impractical to measure any azimuthal dependence. We recall that in pure UPd₃, the (103) peak is still observable up to $T \sim 10$ K¹³, but much broader than below T_0 , indicating short range order.

IV. CONCLUSIONS

In U(Pd_{0.995}Pt_{0.005})₃, bulk measurements reveal two transitions which, due to the similarities in the forms of the anomalies, we associate with the T_{-1} and T_2 transitions in pure UPd₃. Through the energy and polarisation dependence of the observed X-ray resonant scattering, two transitions are identified as being between different phases with long range order of the $5f$ uranium quadrupole moments, at $T_0 = 4.2$ K and $T_{-1} = 4.1$ K. Below T_0 , the azimuthal dependence of the (103) reflection implies a complex combination of quadrupole moments, similar to that in UPd₃ in the same phase, whilst below T_{-1} measurements of the (104) reflection show an in-phase stacking of Q_{xy} quadrupoles along the c -axis.

When the platinum content is increased to 1% the data differs significantly from that of pure UPd₃. Bulk measurements show only broad features, with an anomaly at $T = 2.7$ K. Regrettably it is not possible to stabilise the dilplex cryostat below this temperature to undertake X-ray resonant scattering experiments. However, X-ray resonant scattering reveals short range order below $T^* = 9.2$ K where the correlation lengths are so small as to be undetectable in bulk measurements.

In conclusion, we have determined that long range quadrupolar order in U(Pd_{1-x}Pt_x)₃ is destroyed by less than 1% doping, which is made even more unusual by the fact that this is doping on the ligand site rather than the $5f$ sites which remain unperturbed. This demonstrates the significance of the band structure to the quadrupolar order, since it can be destroyed by a very small increase in the delocalisation of the $5f$ electrons through hybridisation with the Pt $5d$ electrons.

Acknowledgments

HCW and MDL thank the UK Engineering and Physical Sciences Research Council for financial support. We are grateful to D. S. Grachtrup and M. Schäpers for their help with the resistivity measurements. SS acknowledges financial support by the DFG under contract No. SU229/1-3. Work at Brookhaven was supported by the U.S. Department of Energy, Division of Materials Science, under Contract No. DE-AC02-98CH10886.

-
- ¹ G. Zwirgagl and P. Fulde, *J. Phys.: Condensed Matter* **15**, S1911 (2003).
 - ² H. H. Hill, *Plutonium 1970 and Other Actinides* (1970), vol. 17 of *Nuclear Metallurgy*, p. 13.
 - ³ W. J. L. Buyers et al., *Physica B+C* **102**, 291 (1980).
 - ⁴ K. A. McEwen, H. C. Walker, M. D. Le, D. F. McMorrow, E. Colineau, F. Wastin, S. B. Wilkins, J.-G. Park, R. I. Bewley, and D. Fort, *J. Magn. Magn. Mater.* **310**, 718 (2007).
 - ⁵ G. R. Stewart, Z. Fisk, J. O. Willis, and J. L. Smith, *Phys. Rev. Lett.* **52**, 679 (1984).
 - ⁶ L. Petit, A. Svane, W. M. Temmerman, and Z. Szotek, *Phys. Rev. Lett.* **88**, 216403 (2002).
 - ⁷ N. Lingg, D. Maurer, V. Müller, and K. A. McEwen, *Phys. Rev. B* **60**, R8430 (1999).
 - ⁸ S. W. Zochowski, M. de Podesta, C. Lester, and K. A. McEwen, *Physica B* **206-207**, 489 (1995).
 - ⁹ Y. Tokiwa, K. Sugiyama, T. Takeuchi, M. Nakashima, R. Settai, Y. Inada, Y. Haga, E. Yamamoto, K. Kindo, H. Harima, et al., *J. Phys. Soc. Japan* **70**, 1731 (2001).
 - ¹⁰ H. C. Walker, K. A. McEwen, D. F. McMorrow, S. B. Wilkins, F. Wastin, E. Colineau, and D. Fort, *Phys. Rev. Lett.* **97**, 137203 (2006).
 - ¹¹ K. A. McEwen, M. Ellerby, and M. de Podesta, *J. Magn. Magn. Mater.* **140-144**, 1411 (1995).
 - ¹² S. W. Zochowski and K. A. McEwen, *Physica B* **199-200**, 416 (1994).
 - ¹³ D. F. McMorrow, K. A. McEwen, U. Steigenberger, H. M. Rønnow, and F. Yakhov, *Phys. Rev. Lett.* **87**, 057201 (2001).
 - ¹⁴ H. C. Walker, K. A. McEwen, M. D. Le, L. Paolasini, and D. Fort, *J. Phys.: Condensed Matter* **20**, 395221 (2008).
 - ¹⁵ K. A. McEwen, J.-G. Park, A. J. Gipson, and G. A. Gehring, *J. Phys.: Condensed Matter* **15**, S1923 (2003).
 - ¹⁶ The (103) reflection in the orthorhombic notation is equivalent to (1/2 0 3) indexed in the hexagonal notation. All reflections and directions given in this paper are indexed using the orthorhombic cell.
 - ¹⁷ H. C. Walker, K. A. McEwen, P. Boulet, E. Colineau, J.-C. Griveau, J. Rebizant, and F. Wastin, *Phys. Rev. B* **76**, 174437 (2007).
 - ¹⁸ G. R. Stewart and A. L. Giorgi, *J. Low Temp. Phys.* **59**, 185 (1985).
 - ¹⁹ A. de Visser, J. C. P. Klaasse, M. van Sprang, J. J. M. Franse, A. Menovsky, T. T. M. Palstra, and A. Dirkmaat, *Phys. Lett. A* **113**, 489 (1986).
 - ²⁰ A. de Visser, A. Menovsky, and J. J. M. Franse, *Physica B* **147**, 81 (1987).
 - ²¹ R. J. Keizer, A. de Visser, M. J. Graf, A. A. Menovsky, and J. J. M. Franse, *Phys. Rev. B* **60**, 10527 (1999).
 - ²² A. de Visser, M. J. Graf, P. Estrela, A. Amato, C. Baines, D. Andreica, F. N. Gyax, and A. Schenck, *Phys. Rev. Lett.* **85**, 3005 (2000).
 - ²³ D. Fort, *Rev. Sci. Instrum.* **68**, 3504 (1997).
 - ²⁴ M. D. Le, K. A. McEwen, M. Rotter, M. Doerr, A. Barcza, J.-G. Park, R. I. Bewley, J. Brooks, E. Jobilong, and D. Fort, to be published.
 - ²⁵ L. Paolasini, C. Detlefs, C. Mazzoli, S. Wilkins, P. P. Deen, A. Bombardi, N. Kernavanois, F. de Bergevin, F. Yakhov, J. P. Valade, et al., *J. Synch. Rad.* **14**, 301 (2007).
 - ²⁶ Unpublished.
 - ²⁷ L. Paolasini, S. Di Matteo, P. P. Deen, S. Wilkins, C. Mazzoli, B. Detlefs, G. Lapertot, and P. Canfield, *Phys. Rev. B* **77**, 094433 (2008).
 - ²⁸ M. Blume and D. Gibbs, *Phys. Rev. B* **37**, 1779 (1988).